

# Equation of motion coupled-cluster cumulant approach for intrinsic losses in x-ray spectra

Cite as: J. Chem. Phys. **152**, 174113 (2020); <https://doi.org/10.1063/5.0004865>

Submitted: 17 February 2020 . Accepted: 14 April 2020 . Published Online: 06 May 2020

J. J. Rehr , F. D. Vila , J. J. Kas, N. Y. Hirshberg, K. Kowalski , and B. Peng 



View Online



Export Citation



CrossMark

## ARTICLES YOU MAY BE INTERESTED IN

Analytical nuclear gradients for electron-attached and electron-detached states for the second-order algebraic diagrammatic construction scheme combined with frozen-density embedding

The Journal of Chemical Physics **152**, 174109 (2020); <https://doi.org/10.1063/5.0002851>

e<sup>T</sup> 1.0: An open source electronic structure program with emphasis on coupled cluster and multilevel methods

The Journal of Chemical Physics **152**, 184103 (2020); <https://doi.org/10.1063/5.0004713>

Recent developments in the general atomic and molecular electronic structure system

The Journal of Chemical Physics **152**, 154102 (2020); <https://doi.org/10.1063/5.0005188>

Lock-in Amplifiers  
up to 600 MHz



# Equation of motion coupled-cluster cumulant approach for intrinsic losses in x-ray spectra

Cite as: J. Chem. Phys. 152, 174113 (2020); doi: 10.1063/5.0004865

Submitted: 17 February 2020 • Accepted: 14 April 2020 •

Published Online: 6 May 2020



View Online



Export Citation



CrossMark

J. J. Rehr,<sup>1,a)</sup> F. D. Vila,<sup>1</sup> J. J. Kas,<sup>1</sup> N. Y. Hirshberg,<sup>1</sup> K. Kowalski,<sup>2</sup> and B. Peng<sup>2</sup>

## AFFILIATIONS

<sup>1</sup>Department of Physics, University of Washington Seattle, Seattle, Washington 98195, USA

<sup>2</sup>Physical Sciences Division, Battelle, Pacific Northwest National Laboratory, K8-91, PO Box 999, Richland, Washington 99352, USA

<sup>a)</sup> Author to whom correspondence should be addressed: [jjr@uw.edu](mailto:jjr@uw.edu)

## ABSTRACT

We present a combined equation of motion coupled-cluster cumulant Green's function approach for calculating and understanding intrinsic inelastic losses in core level x-ray absorption spectra (XAS) and x-ray photoemission spectra. The method is based on a factorization of the transition amplitude in the time domain, which leads to a convolution of an effective one-body absorption spectrum and the core-hole spectral function. The spectral function characterizes intrinsic losses in terms of shake-up excitations and satellites using a cumulant representation of the core-hole Green's function that simplifies the interpretation. The one-body spectrum also includes orthogonality corrections that enhance the XAS at the edge.

Published under license by AIP Publishing. <https://doi.org/10.1063/5.0004865>

## I. INTRODUCTION

Calculations of x-ray absorption spectra (XAS)  $\mu(\omega)$  from a deep core level of a many-electron system typically begin with Fermi's golden rule,

$$\mu(\omega) = \sum_F |\langle \Psi | D | \Psi_F \rangle|^2 \delta(E_F - E_0 - \hbar\omega), \quad (1)$$

where  $|\Psi\rangle$  is the ground state with energy  $E_0$ ,  $D = \sum_i d_i$  is the many-particle (dipole) interaction with the x-ray field of frequency  $\omega$ , and the sum is over the eigenstates  $|\Psi_F\rangle$  of the many-body Hamiltonian  $H$  with energies  $E_F$ . While full calculations are generally intractable, the problem can be simplified in various ways. For example, in the determinantal  $\Delta$ SCF approach, where the initial and final many-body states are restricted to single-Slater determinants, the final states can be classified in terms of successive single-, double-, and higher  $n$ -tuple excitations.<sup>1,2</sup> Alternatively, with Green's function methods, the summation over final states is implicit.<sup>3-5</sup> For molecular systems, for example, numerous equation of motion coupled-cluster (EOM-CC) approaches have been developed both in energy-space<sup>6,7</sup> and in real time.<sup>8-18</sup> While these developments generally

focus on accurate calculations, relatively less attention has been devoted to the analysis and understanding of many-body effects in the spectra.

Our aim here is to address this shortcoming. To this end, we introduce an alternative approach that combines a real-time EOM-CC method with a cumulant representation of the core-hole Green's function. Cumulant techniques have been increasingly used to understand correlation effects and excited states.<sup>19-21</sup> They also provide an efficient method for calculations of inelastic losses that simplifies their analysis and can be systematically improved. A key step in this approach is a factorization of the XAS transition amplitude,

$$\mu(t) = \langle \Psi | D(0) D(t) | \Psi \rangle = L(t) G_c(t), \quad (2)$$

into an effective one-body transition amplitude  $L(t)$  and the core-hole Green's function  $G_c(t)$ . This strategy is similar to that in the time-correlation approach of Nozières and De Dominicis<sup>22</sup> and the corresponding determinantal approach of Nozières and Combescot<sup>23</sup> (NC) for the edge-singularity problem. As a consequence, the XAS is given by a convolution of a one-electron cross section  $\mu_1(\omega)$  and the core-hole spectral function  $A_c(\omega)$ ,

which are obtained from the Fourier transforms of  $L(t)$  and  $G_c(t)$ , respectively,

$$\mu(\omega) = \int d\omega' \mu_1(\omega - \omega') A_c(\omega'). \quad (3)$$

The intrinsic inelastic losses due to the sudden creation of the core hole lead to shake-up effects characterized by the satellite structure in the spectral function  $A_c(\omega)$  and are directly related to x-ray photoemission spectra (XPS). The one-body spectrum  $\mu_1(\omega)$  also accounts for edge-enhancement orthogonality corrections, analogous to the prediction of Mahan.<sup>24</sup> However, the present approach ignores extrinsic losses and interference that may likely decrease these effects.

In the remainder of this paper, Sec. II describes the EOM-CC approach, and Sec. III describes the application to the XAS. Finally, Secs. IV and V present prototypical results for a simple molecular system and a brief summary, respectively. Some additional details and an alternative example are given in the [supplementary material](#).

## II. EOM-CC THEORY

Intrinsic inelastic losses in XAS and XPS are implicit in the core-hole Green's function  $G_c(t)$  defined as

$$G_c(t) = -i \langle \Psi_c | e^{i(H-E_0)t} | \Psi_c \rangle \theta(t). \quad (4)$$

Here,  $|\Psi_c\rangle = c_c |\Psi\rangle$  is the  $N - 1$ -particle state created by the electron annihilation operator  $c_c$  at  $t = 0^+$  with a core hole in a deep core spin-orbital  $|c\rangle$ ,  $H$  is the many-body Hamiltonian, and  $E_0$  is the ground state energy. Our approach for calculating  $G_c(t)$  is based on the time-dependent EOM-CC ansatz introduced by Schönhammer and Gunnarsson (SG),<sup>25</sup> where  $|\Psi\rangle$  and  $|\Psi_c\rangle$  are taken to be single-Slater determinants. The evolution of  $|\Psi_c(t)\rangle$  is done by transforming to an initial value problem and propagating according to the Schrödinger EOM  $i\partial|\Psi_c(t)\rangle/\partial t = H|\Psi_c(t)\rangle$ , where  $|\Psi_c(0)\rangle = |\Psi_c\rangle$ . The time-evolved state  $|\Psi_c(t)\rangle$  can be defined for any time  $t$  according to a CC ansatz,

$$|\Psi_c(t)\rangle \equiv N_c(t) e^{T_c(t)} |\Psi_c\rangle. \quad (5)$$

For a non-interacting Hamiltonian, the CC ansatz for single-excitations is justified by the Thouless theorem.<sup>26</sup> Here,  $N_c(t)$  is a normalization factor, and the time-dependent CC operator  $T_c(t)$  is defined in terms of single, double, etc., excitation creation operators  $a_n^\dagger$ , i.e.,

$$T_c(t) = \sum_n t_n(t) a_n^\dagger, \quad (6)$$

for example, for the singles,  $n = (a, i)$  and  $a_n^\dagger = c_a^\dagger c_i$ ; and for the doubles,  $n = a, b, j, i$  and  $a_n^\dagger = c_a^\dagger c_b^\dagger c_j c_i$ . Following the CC convention, the indices  $i, j$  refer to occupied,  $a, b, \dots$  to unoccupied, and  $p, q, \dots$  to either occupied or unoccupied levels of the independent particle ground state.

Next, by applying the Schrödinger EOM, left multiplying by  $e^{-T_c(t)}$ , and dividing by  $N_c(t)$  yields the coupled EOM<sup>25</sup>

$$\left[ \frac{i\partial \ln N_c(t)}{\partial t} + \frac{i\partial T_c(t)}{\partial t} \right] |\Psi_c\rangle = \tilde{H}(t) |\Psi_c\rangle, \quad (7)$$

where  $\tilde{H}(t) = e^{-T_c(t)} H(t) e^{T_c(t)}$  is the CC similarity transformed Hamiltonian. On applying successive commutation relations, the expansion of  $\tilde{H}(t)$  terminates after two (four) terms for single-particle (two-particle) operators. Then, left multiplying by  $\langle \Psi_c |$  or  $\langle n | = \langle \Psi_c | a_n$  separates the EOM as

$$i\partial \ln N_c(t) / \partial t = \langle \Psi_c | \tilde{H}(t) | \Psi_c \rangle, \quad (8)$$

$$i\partial t_n(t) / \partial t = \langle n | \tilde{H}(t) | \Psi_c \rangle. \quad (9)$$

Since, for  $m \neq 0$ , the  $[T_c(t)]^m$  terms of the series expansion of  $e^{T_c(t)}$  create excited states orthogonal to  $\langle \Psi_c |$ ,  $\langle \Psi_c | [T_c(t)]^m | \Psi_c \rangle = 0$  for  $m \neq 0$ , and  $G_c(t)$  is simply proportional to the normalization factor,

$$G_c(t) = -i N_c(t) \langle \Psi_c | e^{T_c(t)} | \Psi_c \rangle e^{-iE_0 t} \theta(t) = -i N_c(t) e^{-iE_0 t} \theta(t). \quad (10)$$

Moreover, Eq. (8) implies that  $N_c(t)$  is a pure exponential so that  $G_c(t)$  has a cumulant representation  $G_c(t) = G_c^0(t) e^{C(t)}$ , where  $G_c^0(t) = -i e^{-i\epsilon_c t} \theta(t)$ . Here, the cumulant is

$$C(t) = -i \int_0^t dt' \langle \Psi_c | (\tilde{H}(t') - E'_0) | \Psi_c \rangle, \quad (11)$$

where  $E'_0 = E_0 - \epsilon_c$ .  $C(t)$  can also be represented in the Landau form,<sup>27</sup> which simplifies its interpretation (see Sec. IV),

$$C(t) = \int d\omega \frac{\beta(\omega)}{\omega^2} [e^{i\omega t} - i\omega t - 1], \quad (12)$$

$$\beta(\omega) = \frac{1}{\pi} \text{Re} \int_0^\infty dt e^{-i\omega t} \frac{d}{dt} \langle \Psi_c | \tilde{H}(t) | \Psi_c \rangle. \quad (13)$$

The cumulant kernel  $\beta(\omega)$  accounts for the transfer of the oscillator strength from the main peak to excitations at frequencies  $\omega$ , and the initial conditions  $C(0) = C'(0) = 0$  guarantee its normalization and an invariant centroid at  $-\epsilon_c$ . Next, we evaluate the cumulant in Eq. (11). Our calculations for core-level x-ray spectra are based on an approximate Hamiltonian

$$H = \sum_{pq} f_{pq} \{ c_p^\dagger c_q \} + \frac{1}{2} \sum_{ijab} v_{ijab}^{aj} \{ (c_b^\dagger c_j)^\dagger (c_a^\dagger c_i) \} + E'_0. \quad (14)$$

Here,  $f_{pq} = \epsilon_p \delta_{pq} - v_{pc}^{qc}$  are elements of the Fock operator associated with the core-excited  $N - 1$  particle determinant  $|\Psi_c\rangle$ ,  $\epsilon_p$  are the single-particle ground state energy eigenvalues,  $v_{pc}^{qc}$  is the bare core-hole interaction obtained from standard two-particle antisymmetrized integrals over the  $p, q$ , and  $c$  orbitals, and  $\{\}$  indicates normal ordering with respect to the  $|\Psi_c\rangle$  configuration. The second term in  $H$  approximates valence polarization effects that screen the core hole with interaction coefficients obtained from the two-particle antisymmetrized integrals  $v_{ib}^{aj}$ . In order to illustrate the approach here, we restrict the CC operator  $T_c(t)$  to single-excitations  $T_c(t) = \sum_{ai} t_{ai}(t) c_a^\dagger c_i$ . On applying the commutation relations for  $[H, T]$  with Fermion anticommutation properties, one obtains

$$\langle \Psi_c | (\tilde{H}(t) - E'_0) | \Psi_c \rangle = \sum_{ia} \left[ f_{ia} t_{ai}(t) - \frac{1}{2} \sum_{bj} v_{ib}^{aj} t_{ai}(t) t_{bj}(t) \right]. \quad (15)$$

The non-linear (NL) term in Eq. (15) improves the calculations by shifting the position of the quasiparticle peak and reducing the satellite intensity from that predicted by just the linear (L) first term. From Eq. (9), the coefficients  $t_{ai}(t)$  obey a first order non-linear differential equation,<sup>25</sup>

$$i \frac{\partial t_{ai}}{\partial t} = \langle ai | \bar{H}(t) | \Psi_c \rangle = f_{ai} + \sum_b f_{ab} t_{bi}(t) - \sum_j t_{aj}(t) f_{ji} - \sum_{bj} t_{aj}(t) f_{jb} t_{bi}(t) + \sum_{jb} v_{ib}^{aj} t_{bi}(t). \quad (16)$$

This expression can be interpreted perturbatively as a succession of first order, second order, and third order terms in the off-diagonal matrix elements of  $H$ . The leading term in the cumulant  $f_{ia} t_{ia}^1(t)$  corresponds to a linear response and is second order in the core-hole interaction  $v_{pc}^{qc}$ . The leading amplitude  $t_{ia}^1(t)$  can be evaluated analytically to first order, yielding  $t_{ia}^1(t) = i(f_{ai}/\omega_{ai})[e^{i\omega_{ai}t} - 1]$ , where  $\omega_{ai} = \varepsilon_a - \varepsilon_i$ . Inserting this result into Eq. (11), we obtain an expression for  $C(t)$  valid to second order in the interaction  $f$ ,

$$\beta(\omega) = \sum_{ia} |f_{ia}|^2 \delta(\omega - \omega_{ia}). \quad (17)$$

For comparison, we note that the core-hole spectral function can also be obtained from a  $\Delta$ SCF determinantal approach,<sup>23</sup> where

$$G_c(t) = \det u_{ij}(t), \quad (i, j) = 1, 2, \dots, N \quad (18)$$

and  $u_{ij}(t) = \langle \varphi_i | \varphi_j(t) \rangle e^{-i\varepsilon_i t} = \langle i | e^{i(h' - \varepsilon_i)t} | j \rangle$  are time-dependent overlap integrals, with  $h'$  being the one-particle Hamiltonian for the final state with the core hole.

### III. X-RAY SPECTRA

The contribution to the XAS from a deep core level  $|c\rangle$  is obtained using the time-correlation function with the factorization  $\mu(t) = L(t)G_c(t)$  in Eq. (2). The core-hole Green's function  $G_c$  is obtained from Eqs. (10)–(13). Calculations of the one-body transition amplitude  $L(t)$  can be done in various ways, e.g., using coupled EOM or equivalent integral equations<sup>28–30</sup> or a time evolution based on the overlap integrals  $u_{ij}(t)$ .<sup>23</sup> Here, we use a strategy similar to that of NC, except for the replacement of the sums over  $k$  with the complete set of eigenstates  $\kappa$  of the final state one-particle Hamiltonian  $h' = \sum_{\kappa} \varepsilon_{\kappa} c_{\kappa}^{\dagger} c_{\kappa}$ . Thus, defining the core transition operator  $D = \sum_{\kappa} M_{c\kappa} c_{\kappa}^{\dagger} c_c$ , where  $M_{c\kappa} = \langle c | d | \kappa \rangle$ ,  $L(t)$  becomes

$$L(t) = \sum_{\kappa, \kappa'} M_{c\kappa}^* M_{c\kappa'} L_{\kappa, \kappa'}(t), \quad (19)$$

$$L_{\kappa, \kappa'}(t) = e^{i\varepsilon_{\kappa} t} [u_{\kappa, \kappa'}(t) - \sum_{ij}^{occ} u_{\kappa i}(t) u_{ij}^{-1}(t) u_{j\kappa'}(t)]. \quad (20)$$

The contribution to  $L_{\kappa, \kappa'}(t)$  from the first term on the right-hand side of Eq. (20) leads to the independent particle transition amplitude calculated in the presence of a core-hole  $L_0(t) = \sum_{\kappa} |M_{c\kappa}|^2 \exp(i\varepsilon_{\kappa} t)$  and is consistent with the final-state rule.<sup>31</sup> The diagonal contributions  $\kappa = \kappa'$  of the second term in Eq. (20) contain the analog of a theta function  $\theta(k_F - \kappa)$  that suppresses transitions to the occupied subspace  $\kappa < k_F$ . The off-diagonal contributions to  $L_{\kappa, \kappa'}(t)$

are dominated by  $\kappa$  (or  $\kappa'$ )  $> k_F$  and  $\kappa'$  (or  $\kappa$ )  $< k_F$ , respectively. The net result can be approximated by the compact expression

$$L(t) \approx \sum_{\kappa} |\tilde{M}_{c\kappa}|^2 e^{i\varepsilon_{\kappa} t}, \quad (21)$$

which is equivalent to that derived by Friedel<sup>32</sup> and preserves the XAS sum-rule  $\int d\omega \mu(\omega) = L(0)$ . Here,  $\tilde{M}_{c\kappa} = \langle c | d \bar{P} | \kappa \rangle$ , where  $\bar{P} = 1 - \sum_{i=1}^N |i\rangle \langle i|$  is the projection operator onto the unoccupied valence levels of the ground state. This approximation greatly simplifies the calculation of the XAS, and we have verified that it agrees well with that using Eq. (21). The additional terms  $-\sum_i \langle c | d | i \rangle \langle i | \kappa \rangle$  from  $\bar{P}$  are termed *replacement transitions*.<sup>32</sup> Physically, they serve to cancel transitions to the occupied levels of the initial system. To first order in perturbation theory, the overlap  $\langle i | \kappa \rangle \approx -f_{ik}/\omega_{ik}$  is negative for an attractive core-hole potential and  $\kappa > i$ . Thus, they yield an intrinsic edge enhancement factor  $(1 + \chi_{\kappa})$  for each level  $\kappa$  in the XAS, where  $\chi_{\kappa} \approx -2 \sum_{i=1}^N (M_{ci}/M_{c\kappa}) \langle i | \kappa \rangle$ . While non-singular in molecular systems, this edge-enhancement effect leads to the Mahan power-law singularity in metallic systems,<sup>24</sup>  $\mu_1 \sim |(\varepsilon - \varepsilon_F)/\varepsilon_F|^{-2\delta/\pi}$ . Finally, the XAS in Eq. (3) is obtained by convolving  $\mu_1(\omega)$  with  $A_c(\omega)$ . For convenience, we have shifted both  $\mu_1(\omega)$  and  $A_c(\omega)$  by the core level energy  $\varepsilon_c$ , i.e., with  $\omega = \varepsilon - \varepsilon_c$ , so that in the absence of interactions,  $\mu_1(\omega)$  agrees with the independent particle XAS. This shifted spectral function represents the spectrum of shake-up excitations,

$$A_c(\omega) = \sum_n |S_n|^2 \delta(\omega - \varepsilon_n), \quad (22)$$

where  $S_n = \langle \Psi_c | \Psi'_n \rangle$  is an  $N - 1$  body overlap integral and  $\varepsilon_n = E'_n - E_0$  is the net shake-up energy. The effect of  $A_c(\omega)$  leads to broadening and a significant reduction in the magnitude of the XAS near

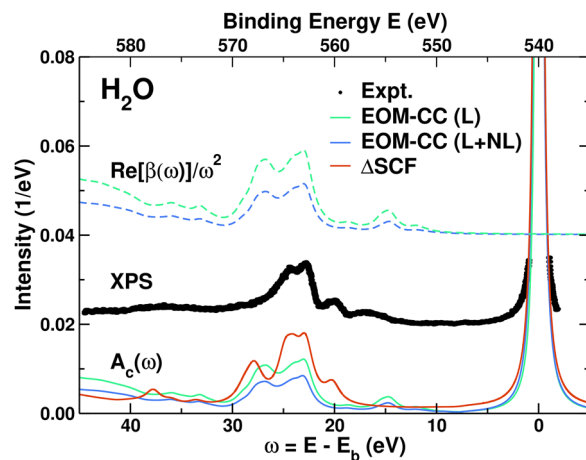


**FIG. 1.** Core spectral function  $A_c(\omega)$  (full lines) and cumulant kernel  $\beta(\omega)$  (dashed lines) computed with only the linear (L) and both linear and nonlinear (L+NL) terms of the EOM-CC cumulant [Eq. (15)] for the  $\text{H}_2\text{O}$  molecule vs absolute binding energy  $E$  or excitation energy  $\omega = E - E_b$  relative to the core binding energy  $E_b = 539.79$  eV.<sup>33</sup> For comparison, the spectral function from the  $\Delta$ SCF method in Eq. (18) and from the experimental XPS (dots)<sup>33</sup> is also shown. To facilitate comparison with the experiment, the EOM-CC and  $\Delta$ SCF calculations include scissors shifts of 15 eV and 7 eV, respectively.

the edge; in metallic systems, it leads to an Anderson power-law singularity<sup>22</sup>  $[(\epsilon - \epsilon_F)/\epsilon_F]^\alpha$ . This effect is opposite in sign and thus competes with the enhancement from  $\mu_1(\omega)$ . The XPS photocurrent is roughly proportional to the spectral function  $J_k(\omega) \sim A_c(\omega - \epsilon_k)$  and is usually measured vs photoelectron energy  $\epsilon_k$  at fixed photon energy  $\omega$ . Thus, the peaks in the XPS correspond to excitations at larger binding energies, as illustrated in Fig. 1.

#### IV. CALCULATIONS

As an example, we present calculations for a free H<sub>2</sub>O water molecule for which both XPS and XAS data are available. All calculations were performed using the experimental gas phase geometry with an OH bond of 0.9578 Å and an HOH angle of 104.48°.<sup>35</sup> We use the aug-cc-pVDZ basis set,<sup>36</sup> expanded with a single set of diffuse *s* and *p* basis functions with exponents 0.0206 and 0.171, respectively, to improve the representation of the Rydberg states. The one-particle effective parameters for the EOM-CC method and the ground state of the  $\Delta$ SCF method of Eq. (19) were obtained from a single-determinant Hartree-Fock reference, while those in the presence of the core hole for the  $\Delta$ SCF method were obtained from a spin-symmetric occupation-constrained Hartree-Fock reference. The results for the cumulant kernel  $\beta(\omega)$  and for the spectral function  $A_c(\omega)$  are shown in Fig. 1 and plotted vs binding energy to compare with the experimental XPS. Note that the peaks in  $\beta(\omega)$  correspond to the inelastic losses in  $A_c(\omega)$ , and for this molecule, they are dominated by shake-up excitations 20–30 eV above the quasiparticle peak. Although our Hartree-Fock based Hamiltonian overestimates their energies, the satellites are in reasonable agreement with those observed in the XPS<sup>33</sup> after scissors corrections are included. From the Landau form of the cumulant, the strength of the main peak is given by the renormalization constant  $Z = \exp(-a) = 0.77$  for the full (L+NL) form of the cumulant in Eq. (15), where  $a = \int d\omega \beta(\omega)/\omega^2 = 0.26$  is the net satellite strength. This is consistent with direct integration over the main peak, which gives  $Z = 0.73$ , and in excellent agreement with the value  $Z = 0.73$  from  $\Delta$ SCF. The quantity  $Z$  is also responsible for the amplitude reduction factor  $S_0^2$  observed in the XAS fine structure.<sup>37</sup> We have checked that our results for  $Z$  agree with those calculated using the energy-space CC Green's function approach.<sup>6,7</sup> In addition, the energy shift  $\Delta = \int d\omega \beta(\omega)/\omega = 19.52$  eV from the middle term in Eq. (12) is the “relaxation energy,” which characterizes correlation corrections to Koopman's theorem for the core binding energy  $E_b = |\epsilon_c| - \Delta = 540.38$  eV, in good agreement with experiment at 539.79 eV, or the leading pole in  $A_c(\omega)$  at 539.21 eV.

Calculations of the XAS using the same basis set are shown in Fig. 2. For comparison, we also include both the experimental XAS<sup>34</sup> and the theoretical XAS computed using the half core-hole approach in StoBe-deMon<sup>38</sup> with a BE88PD86 exchange-correlation functional<sup>39,40</sup> and the same diffuse-extended aug-cc-pVDZ basis set. With the exception of the underestimated intensity for the third peak at about -2.5 eV, the overall agreement with experiment is quite good for both peak positions and their relative intensities. Our independent particle XAS  $L_0$  results are also in very good agreement with the StoBe-deMon calculations but slightly red-shifted, consistent with the stronger core hole in our approach. The corrections to the independent particle XAS in both  $L(\epsilon)$  and  $A_c(\epsilon)$  are quite apparent for this molecule, but opposite in sign, with the edge enhancement

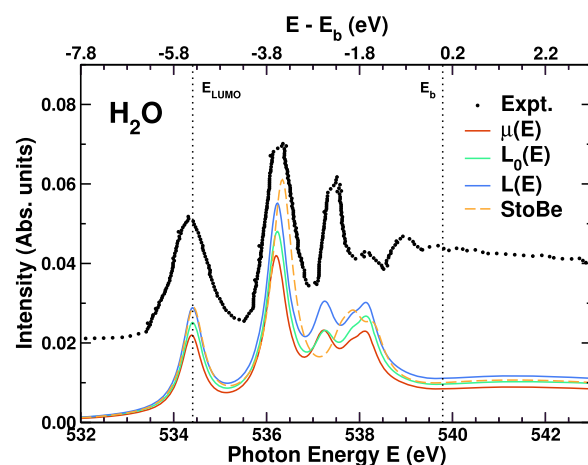


**FIG. 2.** XAS  $\mu(E)$  for H<sub>2</sub>O as a function of photon energy  $E$  from the convolution in Eq. (3) compared to the effective one-electron XAS  $L(E) = \mu_1(E)$ , the independent particle XAS  $L_0(E) = \mu_0(E)$  from the first term in Eq. (21), the independent electron code StoBe with a half-core-hole approximation, and experiment.<sup>34</sup> The O x-ray *K* edge is just below  $E_{\text{LUMO}}$ , and the ionization threshold is at  $E_b$ . To account for the limitations of the basis set in the continuum and facilitate comparison with experiment, the broadening of the spectra above  $E_b$  has been increased to 4 eV.

factor  $1 + \chi$  being about half as strong as the amplitude reduction factor. Given that the first satellites in the spectral function appear 20–30 eV above the quasiparticle peak, any XAS satellite features are expected to fall within the continuum.

#### V. SUMMARY AND CONCLUSIONS

We have presented a combined real-time, EOM-CC approach for calculations of intrinsic losses in XAS and XPS based on the CC ansatz together with the cumulant Green's function representation of the core-hole spectral function. Although additional correlation is possible, for simplicity, we have limited our treatment here to single-determinant wave-functions and an approximate Hartree-Fock based Hamiltonian. The cumulant representation facilitates both calculations and the interpretation of many-body effects in the spectra. A key step in our approach is a time-domain factorization, leading to a convolution formula for the XAS in Eq. (2), in terms of the core-hole spectral function and an effective one-particle spectrum. These quantities account for inelastic losses due to shake-up excitations and edge enhancement corrections due to orthogonality. Although non-singular in molecular systems, both substantially modify the XAS amplitude near the threshold. While extrinsic losses and interference terms due to the coupling of the photo-electron to the core hole are ignored in this treatment, those effects are opposite in sign and tend to cancel. The nature of the CC-EOM cumulant is analogous to that encountered in other theoretical treatments, e.g., using the linked-cluster theorem, field-theoretic methods, or the quasi-boson approximation.<sup>19,22,41</sup> In condensed matter, the cumulant kernel  $\beta(\omega)$  is directly related to the loss function and characterizes excitations such as density fluctuations due to the sudden appearance of the core hole.<sup>41,42</sup> Many extensions of the methodology introduced here are possible. For example, the

treatment of emission spectra is directly analogous to that for the XAS.<sup>23</sup> Additional details are given in the [supplementary material](#). A more extensive treatment including higher order CCSD excitations and additional examples will be presented elsewhere.<sup>43</sup>

## SUPPLEMENTARY MATERIAL

See the [supplementary material](#) for a more detailed discussion of the derivation of Eqs. (4)–(16), as well as results for another example, the diatomic MgO molecule.

## ACKNOWLEDGMENTS

We thank X. Li, J. Lisschner, D. Prendergast, K. Schönhammer, and M. Tzavala for comments and D. Adkins and D. Share for encouragement. This work was supported by the Computational Chemical Sciences Program of the U.S. Department of Energy, Office of Science, BES, Chemical Sciences, Geosciences and Biosciences Division in the Center for Scalable and Predictive Methods for Excitations and Correlated phenomena (SPEC) at PNNL. N.Y.H. acknowledges support from the NSF REU Program in summer 2019.

## DATA AVAILABILITY

The data that support the findings of this study are available from the corresponding author upon reasonable request.

## REFERENCES

- Y. Liang, J. Vinson, S. Pemmaraju, W. S. Drisdell, E. L. Shirley, and D. Prendergast, *Phys. Rev. Lett.* **118**, 096402 (2017).
- Y. Liang and D. Prendergast, *Phys. Rev. B* **100**, 075121 (2019).
- A. J. Lee, F. D. Vila, and J. J. Rehr, *Phys. Rev. B* **86**, 115107 (2012).
- G. F. Bertsch and A. J. Lee, *Phys. Rev. B* **89**, 075135 (2014).
- J. J. Rehr, J. J. Kas, M. P. Prange, A. P. Sorini, Y. Takimoto, and F. Vila, *C. R. Phys.* **10**, 548 (2009).
- B. Peng and K. Kowalski, *Phys. Rev. A* **94**, 062512 (2016).
- B. Peng and K. Kowalski, *J. Chem. Theory Comput.* **14**, 4335 (2018).
- A. F. White and G. K.-L. Chan, *J. Chem. Theory Comput.* **14**, 5690 (2018).
- L. N. Koulias, D. B. Williams-Young, D. R. Nascimento, A. E. DePrince III, and X. Li, *J. Chem. Theory Comput.* **15**, 6617 (2019).
- J. Arponen, *Ann. Phys.* **151**, 311 (1983).
- S. Kvaal, *J. Chem. Phys.* **136**, 194109 (2012).
- T. B. Pedersen and S. Kvaal, *J. Chem. Phys.* **150**, 144106 (2019).
- D. R. Nascimento and A. E. DePrince III, *J. Phys. Chem. Lett.* **8**, 2951 (2017).
- D. R. Nascimento and A. E. DePrince III, *J. Chem. Theory Comput.* **12**, 5834 (2016).
- D. R. Nascimento and A. E. DePrince III, *J. Chem. Phys.* **151**, 204107 (2019).
- D. A. Pigg, G. Hagen, H. Nam, and T. Papenbrock, *Phys. Rev. C* **86**, 014308 (2012).
- T. Sato, H. Pathak, Y. Orimo, and K. L. Ishikawa, *J. Chem. Phys.* **148**, 051101 (2018).
- N. A. Besley, *Chem. Phys. Lett.* **542**, 42 (2012).
- L. Hedin, *J. Phys.: Condens. Matter* **11**, R489 (1999).
- J. S. Zhou, J. J. Kas, L. Sponza, I. Reshetnyak, M. Guzzo, C. Giorgetti, M. Gatti, F. Sottile, J. J. Rehr, and L. Reining, *J. Chem. Phys.* **143**, 184109 (2015).
- J. McClain, J. Lischner, T. Watson, D. A. Matthews, E. Ronca, S. G. Louie, T. C. Berkelbach, and G. K.-L. Chan, *Phys. Rev. B* **93**, 235139 (2016).
- P. Nozières and C. T. De Dominicis, *Phys. Rev.* **178**, 1097 (1969).
- P. Nozières and M. Combescot, *J. Physique* **32**, 11 (1971).
- G. D. Mahan, *Phys. Rev.* **163**, 612 (1967).
- K. Schönhammer and O. Gunnarsson, *Phys. Rev. B* **18**, 6606 (1978).
- D. Thouless, *The Quantum Mechanics of Many-Body Systems* (Academic, New York, 1961).
- L. Landau, *J. Phys. USSR* **8**, 201 (1944).
- D. C. Langreth, *Phys. Rev.* **182**, 973 (1969).
- V. Grebennikov, Y. Babanov, and O. Sokolov, *Phys. Status Solidi (b)* **79**, 423 (1977).
- T. Privalov, F. Gel'mukhanov, and H. Ågren, *Phys. Rev. B* **64**, 165115 (2001).
- U. von Barth and G. Grossmann, *Phys. Rev. B* **25**, 5150 (1982).
- J. Friedel, *Comments Solid State Phys.* **2**, 21 (1969).
- R. Sankari, M. Ehara, H. Nakatsuji, A. De Fanis, H. Aksela, S. L. Sorensen, M. N. Piancastelli, E. Kukk, and K. Ueda, *Chem. Phys. Lett.* **422**, 51 (2006).
- A. Křepelová, J. Newberg, T. Huthwelker, H. Bluhm, and M. Ammann, *Phys. Chem. Chem. Phys.* **12**, 8870 (2010).
- A. R. Hoy and P. R. Bunker, *J. Mol. Spectrosc.* **74**, 1 (1979).
- R. A. Kendall, T. H. Dunning, and R. J. Harrison, *J. Chem. Phys.* **96**, 6796 (1992).
- J. J. Rehr, E. A. Stern, R. L. Martin, and E. R. Davidson, *Phys. Rev. B* **17**, 560 (1978).
- L. Triguero, L. G. M. Pettersson, and H. Ågren, *J. Phys. Chem. A* **102**, 10599 (1998).
- A. D. Becke, *Phys. Rev. A* **38**, 3098 (1988).
- J. P. Perdew and W. Yue, *Phys. Rev. B* **33**, 8800 (1986).
- D. C. Langreth, *Phys. Rev. B* **1**, 471 (1970).
- J. J. Kas and J. J. Rehr, *Phys. Rev. Lett.* **119**, 176403 (2017).
- F. D. Vila, J. J. Rehr, J. J. Kas, B. Peng, and K. Kowalski, UW Preprint (2020).